Evaluation of early bone response to fluoride-modified and anodically oxidized titanium implants through continuous removal torque analysis

AUTHORS: Taek-Ka Kwon[1*], DDS, MSD, PhD, Hyo-Jung Lee[2*], DDS, MSD, PhD, Seung-Ki Min[3], DDS, MSD, In-Sung Yeo[4], DDS, MSD, PhD

ABSTRACT: **(171 words)**

Purpose: The purpose of this study was to compare between a bioactive and a bioinert implant with different geometries by continuous measurement of the removal torque and calculation of the angular momentum of each surfaced implant.

Materials and Methods: Six New Zealand white rabbits were employed in the study. Each rabbit received two implants. A bioactive fluoride-modified implant with a conical connection and microthread design was inserted into one tibia, and a bioinert anodically oxidized implant with an external connection design was inserted into the other. After 2 weeks of implant insertion, the removal torque values were continuously measured according to time. Using the time-torque curve resulting from the measurements, the maximum values were determined and the angular momenta were calculated.

Results: The anodically oxidized implant had significantly higher peak removal torque and angular momentum values than the fluoride-modified implant (P < 0.05).

Conclusions: The impact of the fluoride-modified bioactive implant on early bone response remains unclear. Considering the angular momentum of dental implants may assist in elucidation of the effect of implant geometry on bone response.

KEYWORDS: Implant design, biomechanics, surface modification, implant interface, bioactive material

[1] Assistant Professor, Dept. of Dentistry, St. Catholic Hospital, Catholic University of Korea, Ji-dong, Paldal-gu, Suwon 442-723, South Korea

[2] Assistant Professor, Section of Dentistry, Seoul National University Bundang Hospital, Gumi-ro, Bundang-gu, Seongnam 463-707, South Korea

[3] Graduate Student, Dept. of Oral and Maxillofacial Surgery, School of Dentistry and Dental Research Institute, Seoul National University, Daehak-ro, Jongno-gu, Seoul 110-749, South Korea

[4] Assistant Professor, Dept. of Prosthodontics, School of Dentistry and Dental Research Institute, Seoul National University, Daehak-ro, Jongno-gu, Seoul 110-749, South Korea

[*] These authors contributed equally to this work.

Reprint requests and correspondence to: In-Sung Yeo, DDS, MSD, PhD, Dept. of Prosthodontics, School of Dentistry, Seoul National University, Daehak-ro, Jongno-gu, Seoul, South Korea, 110-749

Tel: +82-2-2072-2661   Fax: +82-2-2072-3860   E-mail: pros53@snu.ac.kr

Implant geometry and surface properties are important factors for the long-term clinical success of dental implants.[1-3] Surface properties have been modified in a variety of ways to improve the response of the bone that comes into contact with the implant surface.[4-6] Bioactive implant surfaces, which are fluoridated or coated with calcium phosphate, have recently been developed and used in the dental market.[7] A bioactive coating is known to impart bioactivity to an otherwise bioinert material, such as titanium.[8,9] In an earlier study, however, no significant differences were found between the impact of bioactive and bioinert surfaces on early bone response in histomorphometric evaluation.[10] But, there is no previous study to compare these two surfaces in physiocomechanical manners such as removal torque (RT) measurement.

Histomorphometry analyses and RT tests have been commonly performed to evaluate the strength and stability of the implant surface.[11-13] RT measurements were obtained in many previous experiments through the use of a manually operated RT tester. However, manual RT testers have limitations, including irregular angular speed and uneven reverse torque applied in different vectors.[10,13-16] This type of hand-held torque gauge records the maximum torque value only, and as such, there is no way to understand the sequential change around the peak value.

If RT is continuously measured according to time, angular momentum can be calculated by integrating the torque values in a chronological manner. Because angular momentum is expressed as the multiplication of the angular speed and the moment of inertia of a rotating body, it is considered to be another means to evaluate implant geometry and the effect of geometry on the bone-implant interface. Nonetheless, no studies to date have analysed the angular momentum of dental implants by constant assessment of the reverse torque, with the exception of mini-screws used to gain skeletal anchorage in orthodontics.[17]

The purpose of this study was thus to compare a bioactive implant surface with a bioinert surface by continuously measuring the removal torque and calculating the angular momentum of each surfaced implant.

MATERIALS AND METHODS

Sample preparation and implant surface modification

Ten control implants had a bioinert anodised surface and the traditional external connection design (TiUnite®, Nobel Biocare AB, Gothenburg, Sweden). The diameter and length of the control implants were 4.0 mm and 8.5 mm, respectively. Ten test implants had a bioactive fluoride-modified surface and the characteristic conical seal™ and microthreads™ design (Osseospeed™, Astra Tech, Mölndal, Sweden).The diameter and length of the test implants were 4.0 mm and 8.0 mm, respectively. Following fluoride treatment, the surface of the test implants were moderately roughened by grit blasting with titanium dioxide (TiO_2) particles, yielding a turned titanium implant.[9,18] The turned titanium implant was used as an anode in an electrochemical cell to yield an anodically oxidized titanium implant. During this procedure, oxidation takes place at the implant surface when a potential is applied under appropriate conditions. Oxidation provides the implants with a porous oxide surface.[19]

Surface characteristics

Four implants from each group were used for the surface analysis. The analysis was performed using field emission scanning electron microscopy (FE-SEM), energy dispersive spectroscopy (EDS), and confocal laser scanning microscopy (CLSM). An image of the overall surface was provided by FE-SEM (model S-4700, Hitachi, Tokyo, Japan). Analysis of the components and element content of the modified surfaces was performed using EDS (model EX220, Horiba Ltd., Kyoto, Japan). The surface roughness was measured using CLSM (model LSM 5-Pascal, Carl Zeiss AG, Oberkochen, Germany). Three screw-sides from each implant surface were selected at random. Two roughness

parameters, average height deviation, S_a, and developed surface ratio, S_{dr}, were measured. The area of measurement was 300 μm × 300 μm on a 200× magnified image.

Animal surgery

The study was approved by the Animal Research Committee of Seoul National University Bundang Hospital (IACUC protocol approval number: BA0909-050-037-01). Animal selection, management, and preparation and subsequent surgical protocols were performed in accordance with the Institute of Laboratory Animal Resources guidelines of Seoul National University Bundang Hospital.

Six male New Zealand white rabbits approximately 6 months of age and weighing approximately 2.6 to 3 kg were used. The rabbits showed no signs of illness or disease. The rabbits were anaesthetised with an intramuscular injection of tiletamine/zolazepam (Zoletil 50, Virbac Korea Co. Ltd., Seoul, Korea) (15 mg/kg) and xylazine (Rompun, Bayer Korea Ltd., Seoul, Korea) (5 mg/kg). Prior to surgery, the skin over the area of the proximal tibia was shaved and washed with Betadine. Cefazolin (33 mg/kg), a preoperative antibiotic (Yuhan Co., Seoul, Korea), was administered intramuscularly. Lidocaine, a local anaesthetic, was injected into each surgical site. The skin was incised, and each tibia was exposed following muscle dissection and periosteal elevation. The implant sites were prepared on the flat tibia surface using a dental drill and sterile and profuse saline irrigation. The diameter of the final drill hole was 3.7 mm. The implant was inserted into the drill hole and did not contact the lower cortical layer (Fig. 1). Each rabbit received two implants. A fluoride-modified implant (Osseospeed™) was inserted into one tibia, and an oxidized implant (TiUnite®) was inserted into the other. The microthreads of the fluoride-modified implant were visible on the upper cortex. A corresponding portion of the oxidized implant was also visible (Fig. 1). Thus, only the bone response around the macrothreads of each implant was considered. After implant insertion, the cover screws were securely fastened, and the surgical sites were closed in layers. After the surgery, each rabbit received cefazolin (33 mg/kg) by intramuscular injection.

The rabbits were anaesthetised and sacrificed by intravenous administration of potassium chloride after 2 weeks of bone healing.

Continuous RT tests

The implants were exposed by incision and periosteal elevation. They were then surgically removed en bloc with an adjacent bone collar. The cover screw of the implant was removed. The implant within the tibia-implant block was firmly attached to a customised metal mold with a screw, and wax was applied to the exposed threads of the implant. Acrylic resin (liquid and powder) (Ortho-jet, Lang-dental, IL, USA) was mixed and poured into the metal mold. The metal cover was placed on the metal mold containing the resin, and the resin was then cured. The metal cover was removed from the mold, and the tibia-implant-resin assembly was unscrewed from the metal mold. The polymerised acrylic resin made strong contact with the tibia but did not contact the implant threads due to the coating of wax. Then the wax was removed. The tibia-implant-resin block was next used for RT testing in the continuous RT testing apparatus (Fig. 2).

Continuous RT values were measured with a TSTM motorised torque test stand (Mark-10 Co., NY, USA). The angular speed of the reverse torque was 0.3 revolutions per minute (RPM), or 1.8 degrees per second. Figure 2 schematically shows the test method that was employed in this study. During the RT test, implants were subjected to the same long axis of the torque sensor. The authors continuously recorded the torque values for 90 seconds from the time when the reverse torque was applied to the tibia-implant-resin assembly, which resulted in a time-torque curve (Fig. 3). The peak RT was taken from the time-torque curve data. The area below the time-torque curve was calculated from 0 to 90 seconds and represented the total torque area. The area below the curve between 0 seconds and peak torque time was defined as the torque area before the peak (TABP), and the area between peak torque time and 90 seconds was defined as the torque area after the peak (TAAP). The mean torque values before the peak (MTBP) and those after the peak (MTAP) were also calculated by dividing the TABP and TAAP, respectively, by the appropriate times. In the case of the MTBP,

this corresponded to the mean time taken to reach the peak, and in the case of the MTAP, this corresponded to the mean time from the peak to 90 seconds.

Statistics

The independent sample T-test was used to assess the statistical significance of the difference in surface roughness parameters (S_a and S_{dr}) between the test and control implants. The independent T-test was also used to determine statistically significant differences between the two groups in the peak RT, total torque area, and mean torque, while the Mann-Whitney U test was used to determine statistically significant differences in the TABP, MTBP, TAAP, and MTAP. A *p* value of less than 0.05 was considered statistically significant.

RESULTS

Surface characteristics

CLSM analyses of the investigated surfaces demonstrated that all of the implants had moderately roughened surfaces (S_a 1 to 2 μm, Fig. 4). The mean surface roughness values for the anodically oxidized and the fluoride-modified surfaces were both 1.1 μm in S_a. The S_{dr} values of the oxidized and fluoride-modified implants were 39.3% $\pm$ 2.9% and 38.0% $\pm$ 2.3%, respectively. There was no statistical difference in the S_{dr} between the compared surfaces (P > 0.05).

The morphologic evaluation of each surface was performed using FE-SEM (Fig. 5). The macrothread morphology of each implant was relatively similar when observed at 50× magnification. At higher magnification, however, many porous structures were observed to be scattered on the oxidized surface. By contrast, the fluoride-modified surface had a rough, irregular pattern that was produced by grit blasting. Nanostructures were detected on both surfaces at 10,000× magnification. Sharp nano-peaks were observed on the surface of the fluoride-modified implant, while large and small nanopores were visible on the surface of the oxidized implant.

7

EDS analysis showed that the oxidized surface was composed of 86.6% titanium and 13.4% phosphorus by weight. The fluoride-modified surface, on the other hand, was 100% titanium by weight (Table I). No fluoride content was detected by EDS, discussed below.

Continuous RT tests

The loosening patterns of all investigated implants were similar. Each implant firmly resisted the reverse torque and then loosened suddenly, revealing the peak RT. After peak torque was reached, the torque values decreased with little fluctuation (Fig. 6).

Table II shows the results of the continuous RT test for both implant types. After a 2-week healing period, the means and standard deviations of the peak RT values for the oxidized and the fluoride-modified implants were 60.5 Ncm ± 8.8 Ncm and 39.9 Ncm ± 9.3 Ncm, respectively. The peak RT values of the oxidized implant were significantly higher than those of the fluoride-modified implants (P = 0.003). The TABP and MTBP values for the oxidized group, corresponding to parameters before the peak torque value was reached, were also significantly higher than those for the fluoride-modified group (P = 0.016 and P = 0.025, respectively). No significant differences were found in total torque area, mean torque, TAAP, or MTAP between the investigated implants (P > 0.05).

DISCUSSION

There is a general consensus that moderately roughened surfaces lead to a stronger bone response (e.g., more robust bone formation and integration, faster bone healing) compared with turned, milled, or polished surfaces.[7,16,20-22] Increasing numbers of surface modifications continue to be introduced,[20,23-27] and osseointegration promoted by many of these roughened surfaces has been demonstrated to be superior to that afforded by 'machined' titanium surfaces. However, it is unclear

whether, in general, one surface modification is better than another.[10,28-30] Therefore, this study compared two modified surfaces that were not turned.

In contrast to previous studies, this study showed that a bioinert anodised implant had a significantly larger resistance to RT than a bioactive fluoride-modified implant.[8,9] Moreover, the EDS results showed that no fluoride was detected, calling into question the efficiency of the modification methodology. Therefore, one cannot unequivocally address the bioactive effect of fluoride on early bone response, if any, from the data provided in this study. In addition, earlier work detected one atomic percent of fluoride on a fluoride-modified implant and questioned the influence of this small amount of chemical on bone response.[6] However, further study will be required to more conclusively understand the impact of trace amounts of fluoride on early bone response.

This research employed a continuous removal torque tester and recorder. This instrument allowed the authors to observe the change of torque according to time. This study is the first of its type in investigations of the strength and stability of restorative implants. By integrating the continuously measured torque values with time, the authors found that the oxidized implant had higher peak removal torque, torque area before the peak (TABP) and mean torque before the peak (MTBP) values than did the fluoride-modified implant. In addition, the oxidized implant had higher RT values than did the fluoride-modified implant. If the fluoride-modified surface is assumed to promote a superior early bone response (although, as noted above, the bioactive properties of this implant are in question), the implant geometry of the oxidized implant may compensate for the inferior surface. The consideration of angular momentum is important to assess the impact of implant geometry on bone response, because the moment of inertia is determined by the geometry of a body, that is, implant geometry.

CONCLUSION

In conclusion, the angular momentum of an implant, which is resistant to RT, can be calculated via continuous measurement of RT values according to time. The effects of implant geometry and surface properties on bone response can be analysed considering both peak RT and angular momentum. This study compared the osseointegrative potential of a fluoride-modified implant with a bioinert oxidized implant, and determined that oxidized surface showed superior early bone response in physiomechanical aspect. However, given the fluoride detection limitations described herein, the bioactive effects of trace amounts of fluoride on early bone response remain unclear. Further study will be required to more conclusively address this issue.

ACKNOWLEDGEMENTS

DISCLOSURE

REFERENCES

1. Albrektsson T, Branemark PI, Hansson HA, et al. Osseointegrated titanium implants. Requirements for ensuring a long-lasting, direct bone-to-implant anchorage in man. Acta Orthop Scand. 1981;52: 155-170.

2. Kido H, Saha S. Effect of HA coating on the long-term survival of dental implant: a review of the literature. J Long Term Eff Med Implants. 1996;6: 119-133.

3. Steigenga JT, al-Shammari KF, Nociti FH, et al. Dental implant design and its relationship to long-term implant success. Implant Dent. 2003;12: 306-317.

4. Cooper LF. A role for surface topography in creating and maintaining bone at titanium endosseous implants. J Prosthet Dent. 2000;84: 522-534.

5. Ellingsen JE. Surface configurations of dental implants. Periodontol 2000. 1998;17: 36-46.

6. Wennerberg A, Albrektsson T. On implant surfaces: a review of current knowledge and opinions. Int J Oral Maxillofac Implants. 2010;25: 63-74.

7. Albrektsson T, Wennerberg A. Oral implant surfaces: Part 1--review focusing on topographic and chemical properties of different surfaces and in vivo responses to them. Int J Prosthodont. 2004;17: 536-543.

8. Cooper LF, Zhou Y, Takebe J, et al. Fluoride modification effects on osteoblast behavior and bone formation at TiO2 grit-blasted c.p. titanium endosseous implants. Biomaterials. 2006;27: 926-936.

9. Ellingsen JE, Johansson CB, Wennerberg A, et al. Improved retention and bone-tolmplant contact with fluoride-modified titanium implants. Int J Oral Maxillofac Implants. 2004;19: 659-666.

10. Yeo IS, Han JS, Yang JH. Biomechanical and histomorphometric study of dental implants with different surface characteristics. J Biomed Mater Res B Appl Biomater. 2008;87: 303-311.

11. Ferguson SJ, Broggini N, Wieland M, et al. Biomechanical evaluation of the interfacial strength of a chemically modified sandblasted and acid-etched titanium surface. J Biomed Mater Res A. 2006;78: 291-297.

12. Shin D, Blanchard SB, Ito M, et al. Peripheral quantitative computer tomographic, histomorphometric, and removal torque analyses of two different non-coated implants in a rabbit model. Clin Oral Implants Res. 2010.

13. Meredith N. Assessment of implant stability as a prognostic determinant. Int J Prosthodont. 1998;11: 491-501.

14. Ahn S, Vang MS, Yang HS, et al. Histologic evaluation and removal torque analysis of nano- and microtreated titanium implants in the dogs. J Adv Prosthodont. 2009;1: 75-84.

15. Klokkevold PR, Nishimura RD, Adachi M, et al. Osseointegration enhanced by chemical etching of the titanium surface. A torque removal study in the rabbit. Clin Oral Implants Res. 1997;8: 442-447.

16. Koh JW, Yang JH, Han JS, et al. Biomechanical evaluation of dental implants with different surfaces: Removal torque and resonance frequency analysis in rabbits. J Adv Prosthodont. 2009;1: 107-112.

17. Kim SH, Lee SJ, Cho IS, et al. Rotational resistance of surface-treated mini-implants. Angle Orthod. 2009;79: 899-907.

18. Carlsson L, Rostlund T, Albrektsson B, et al. Implant fixation improved by close fit. Cylindrical implant-bone interface studied in rabbits. Acta Orthop Scand. 1988;59: 272-275.

19. Hall J, Lausmaa J. Properties of a new porous oxide surface on titanium implants. Applied Osseointegration Research. 2000;1: 5-8.

20. Albrektsson T, Wennerberg A. Oral implant surfaces: Part 2--review focusing on clinical knowledge of different surfaces. The International journal of prosthodontics. 2004;17: 544-564.

21. Hayakawa T, Yoshinari M, Nemoto K, et al. Effect of surface roughness and calcium phosphate coating on the implant/bone response. Clin Oral Implants Res. 2000;11: 296-304.

22. Shalabi MM, Gortemaker A, Van't Hof MA, et al. Implant surface roughness and bone healing: a systematic review. J Dent Res. 2006;85: 496-500.

23. Buser D, Broggini N, Wieland M, et al. Enhanced bone apposition to a chemically modified SLA titanium surface. J Dent Res. 2004;83: 529-533.

24. Guo J, Padilla RJ, Ambrose W, et al. The effect of hydrofluoric acid treatment of TiO2 grit blasted titanium implants on adherent osteoblast gene expression in vitro and in vivo. Biomaterials. 2007;28: 5418-5425.

25. Kang BS, Sul YT, Oh SJ, et al. XPS, AES and SEM analysis of recent dental implants. Acta Biomater. 2009;5: 2222-2229.

26. Schwarz F, Herten M, Sager M, et al. Bone regeneration in dehiscence-type defects at chemically modified (SLActive) and conventional SLA titanium implants: a pilot study in dogs. J Clin Periodontol. 2007;34: 78-86.

27. Zhao G, Schwartz Z, Wieland M, et al. High surface energy enhances cell response to titanium substrate microstructure. J Biomed Mater Res A. 2005;74: 49-58.

28. Marin C, Granato R, Suzuki M, et al. Removal torque and histomorphometric evaluation of bioceramic grit-blasted/acid-etched and dual acid-etched implant surfaces: an experimental study in dogs. J Periodontol. 2008;79: 1942-1949.

29. Wennerberg A, Albrektsson T. Suggested guidelines for the topographic evaluation of implant surfaces. Int J Oral Maxillofac Implants. 2000;15: 331-344.

30. Wennerberg A, Albrektsson T. Effects of titanium surface topography on bone integration: a systematic review. Clin Oral Implants Res. 2009;20 Suppl 4: 172-184.
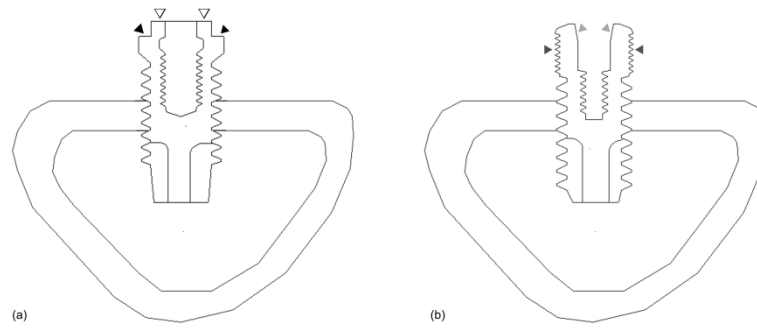
Fig. 1. The cross-sectional views of the implants installed in the rabbit tibia are shown. (a) The anodically oxidized implant has the external hex connection design, which consists of a hex top (black-edged white arrows) and a platform (black arrows). (b) The fluoride-modified implant has the structures of conical seal (light grey arrows) and microthreads (dark grey arrows). Note that both the groups are installed in similar depth and that the microthreads in (b) have no contact with the bone to guarantee that the environments of bone-implant interface in both groups are similar with each other. The inserted implants are only engaged with the upper cortex of the rabbit tibia.
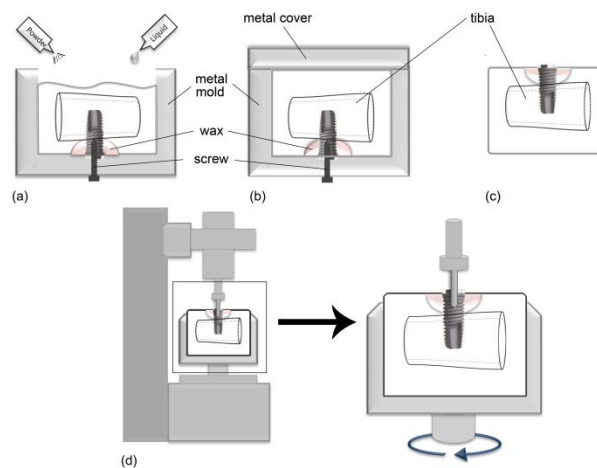
Fig. 2. Schematic diagram of specimen processing in the continuous removal torque test. (a) Acrylic resin powder and liquid were poured over the tibia-implant block which fixed to customized metal (aluminum) mold with the impression coping screw after the exposed implant surface was blocked out with wax. (b) Acrylic resin was polymerized in the customized mold. (c) The tibia-implant-resin assembly was retrieved after the screw and metal mold were removed. (d) The tibia-implant-resin assembly was loaded on the motorized torque test stands, which continuously measured removal

torque values according to time. The upper part was connected to the torque sensor, and the lower part was the motorized table that rotated clockwise 1.8 degrees per second. The diagram in the rectangular area is magnified on the right side to show more in detail. Note the clockwise-rotating lower part (blue arrow), which results in application of the reverse torque to the implant.
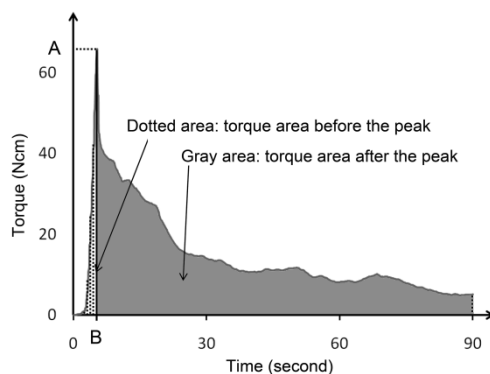

Fig. 3. A time-torque curve resulted from the continuous measurement of RT values according to time. Point A indicates the maximum value of RT, where the osseointegrated implant begins to be reversely rotated. Point B is the time at the peak RT. The dotted area represents the TABP, which means the angular momentum from 0 to point B while the gray area represents the TAAP, which means the angular momentum form point B to 90 seconds.
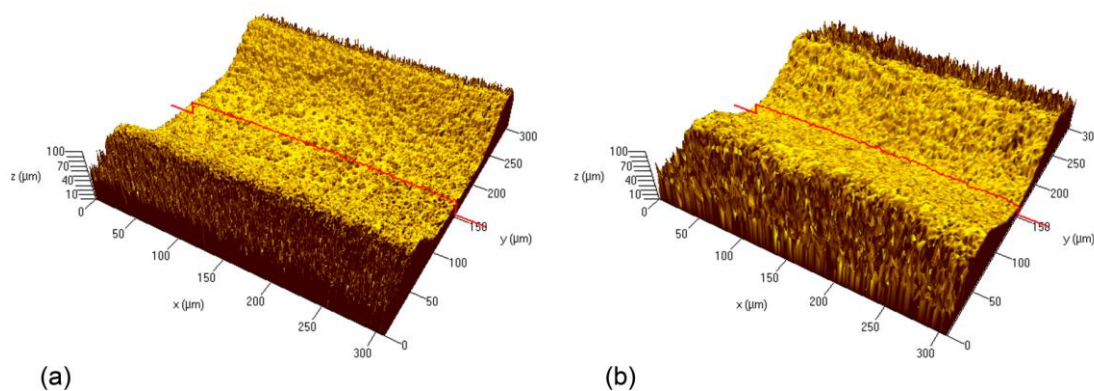

Fig. 4. Valleys of the anodically oxidized surface (a) and the fluoride-modified surface (b) are shown. Although the anodically oxidized surface was different in topography from the fluoride-modified surface, the mean S_a and S_{dr} values of the control implant was similar to those of the test implant.
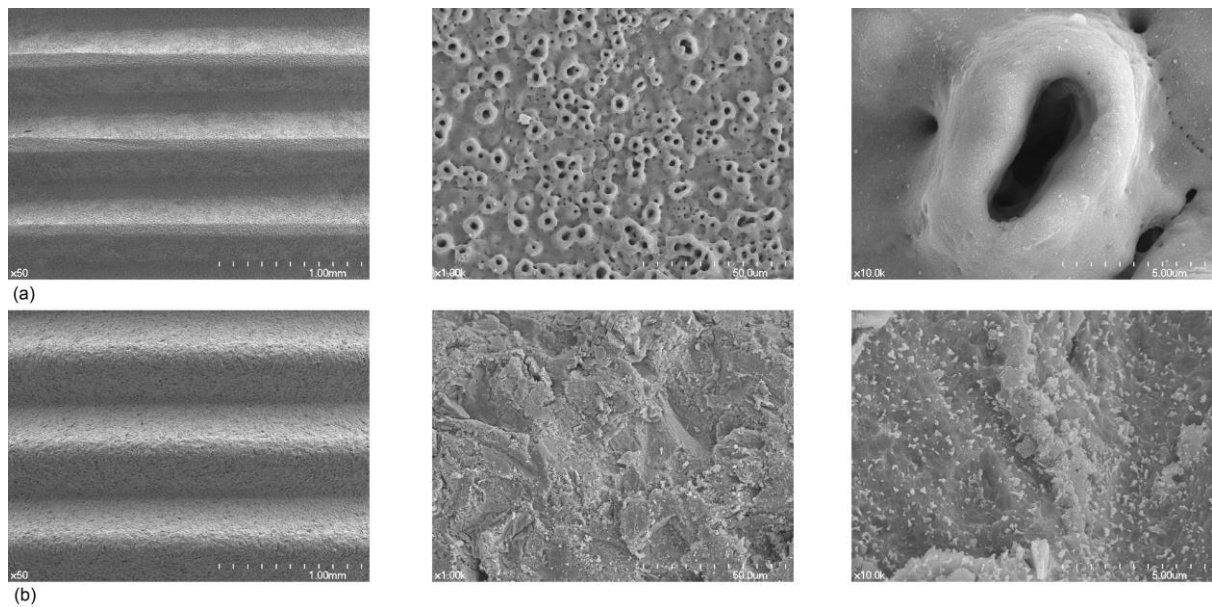
Fig. 5. SEM images of each surface at the different resolutions (50×, 1000×, and 10000× from the left). (a) The anodically oxidized implant has a rough surface showing many micropores with elevated margin that look like volcanoes. Pore size varies between 1 and 10 μm. Many nanopores with orifices of less than 1 μm are also scattered. (b) The fluoride-modified implant has a rough surface with facets produced by blasting. High-power image reveals numerous nanostructures on the surface of the blasted facets.
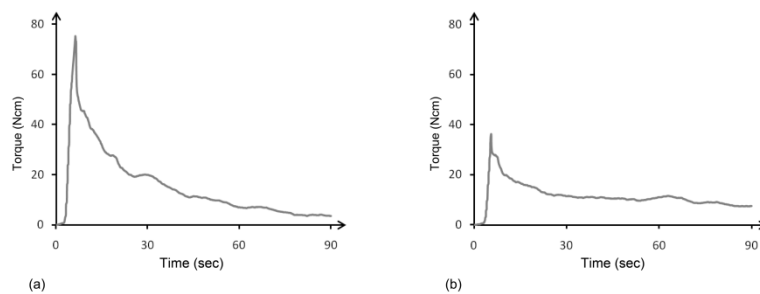

Fig. 6. Typical time-torque curves of the anodically oxidized surface (a) and the fluoride-modified surface (b). The peak removal torque value, TABP and MTBP of the anodically oxidized implant were significantly higher than those of the fluoride-modified implant ($P < 0.05$).